Exp Brain Res (1996) 112:135–146

RESEARCH ARTICLE

D. Straumann · D.S. Zee · D. Solomon · P.D. Kramer

Validity of Listing's law during fixations, saccades, smooth pursuit eye movements, and blinks

Received: 25 September 1995 / Accepted: 16 April 1996

Abstract In its original formulation, Listing's law referred only to eye positions during steady fixation. In recent years, however, several studies have suggested that Listing's law can be extended to the movements of the eyes, including during saccades and smooth pursuit. A major problem in deciding whether or not Listing's law is obeyed *during* eye movements is the influence of any spontaneous fluctuations in torsional eye position. To try to settle this question, the three-dimensional position of the eyes (around the three axes: horizontal, vertical, and torsional) was recorded with dual search coils in five normal subjects during fixations, 20° saccades, blinks, and 20° pursuit movements with a 20°/s stimulus velocity. Eye movements across a wide range of horizontal positions were measured at different elevations of gaze during 11 min. Variability (as reflected in the standard deviation of torsional eye position) was used as a measure of the validity of Listing's law. After linear detrending single trials, each lasting 21.5 s, to remove the effects of drift over minutes, the reduction in the standard deviation of torsional position in tertiary eye positions was 54% assuming a planar and 58% assuming a second-order curved Listing's surface. We attributed this long-term fluctuation of the torsional signal to slippage of the coil on the eye. The remaining variability was mainly due to short-term fluctuation of eye torsion over seconds. The impact of hysteresis, associated with consecutive centrifugal-centripetal horizontal movements, on the variability of torsional eye position appeared negligible. Peak increases in the standard deviation from the fixation baseline after fitting individual Listing's planes for each trial were 348% during blinks, 141% during saccades, and 72% during pursuit movements (median value of five subjects). In conclusion, Listing's law during blinks, saccades, and pursuit is less valid than during fixations, which raises doubts about the existence of an internal "Listing's law operator" for eye movements. Possibly, central eye *velocity* commands do not comply with Listing's law.

Key words Torsion · Three-dimensional eye movements · Donders' law · Listing's law · Human

D. Straumann · D.S. Zee · D. Solomon · P.D. Kramer
Department of Neurology, Johns Hopkins Hospital, Baltimore, Maryland, USA

D. Straumann (✉)
Neurology Department, Zurich University Hospital, CH-8091 Zurich, Switzerland; Tel: +41-1-255-5500, fax: +41-1-255-4507,
E-mail: dominik@neurol. unizh.ch

Introduction

In 1848, Donders published his famous law that states that the torsional orientation of the ocular globe is independent of the path that the eye takes to reach its current position. Later, Listing mathematically specified the function that links the torsional degree of freedom of the eye with gaze direction (Ruete 1853; Helmholtz 1867). According to Listing's law, all axes about which the eye rotates from the reference position to any other position lie in a plane, the so-called Listing's plane, provided the head is stationary. It follows that, if Donders' law is violated, Listing's law also can not be valid.

At the time when Donders' and Listing's laws were formulated, no distinction was made between the different classes of eye movements on the basis of their dynamic properties (Westheimer 1989). These laws were established by the use of afterimages and therefore were meant to apply to the static situation, i.e., during fixations. Recently, however, investigators have tested the validity of Donders' and Listing's laws under dynamic conditions. It was found that the quaternion or rotation vectors of the eye during saccades and smooth pursuit lie *approximately* in a plane (Tweed and Vilis 1990; Straumann et al. 1991; Haslwanter et al. 1991; Tweed et al. 1992; Minken et al. 1993). While the results of these experiments have been consistent among laboratories, the fact that these investigators lumped data from movements of different starting positions, directions, and amplitudes raises questions about their conclusions with re-

spect to the implementation of Donders' and Listing's laws *during* movements.

To check the validity of Listing's law for saccades or smooth pursuit eye movements, one typically pools a number of trajectories between different tertiary positions, fits a plane through the data cloud of rotation or quaternion vectors (Haustein 1989; Tweed and Vilis 1987), and computes the standard deviation of data points from the best-fit plane. On the basis of this value one concludes whether or not Listing's law, and therefore Donders' law, is valid. Typical standard deviations during spontaneous eye movements with saccades and fixations range around 1°; during smooth pursuit eye movements values are smaller (by about 25%) (Haslwanter et al. 1991; Tweed et al. 1992). We still do not know how much of the deviation from an ideal implementation of Listing's law can be accepted as "biological noise".

Listing's law can also be tested by plotting the eye movement component out of Listing's plane during gaze displacements between different orbital positions. For centrifugal and centripetal horizontal saccades at different gaze elevations one finds a consistent pattern of transient movements out of Listing's plane (Straumann et al. 1995): adducting saccades produce intorsional movements when made in downward gaze positions and extorsional movements with upward gaze positions; abducting saccades show torsional movements in the opposite directions. Torsional movements are still continuing at the end of saccades due to a relatively slow drift back to Listing's plane. These transient torsional movements have been named torsional "blips" (Tweed et al. 1994). Schnabolk and Raphan (1994) have suggested that torsional blips arise because saccades are created by a two-dimensional velocity signal with only a horizontal and vertical component. Due to the noncommutative properties of rotations, this velocity signal transiently drives the eyes away from Listing's plane during saccades between nonradial eye positions. The integrated eye position signal, however, complies with Listing's law, according to the model. When applying realistic parameters for the saccadic system (burst, integrator, plant), the modified Schnabolk-Raphan model predicts violations of Listing's law during saccades, which agree with data recorded in humans during horizontal, but not vertical saccades (Straumann et al. 1995). Hence, a finer three-dimensional analysis of saccade trajectories between specific directions of gaze reveals dynamic limitations of Listing's and Donders' laws which could be obscured by pooling eye positions from trajectories with different initial positions, directions, and amplitudes.

The literature on the validity of Listing's law for smooth pursuit eye movements suffers from the same problem. Some authors have published data showing consistent violations of Donders' and Listing's laws during pursuit movements (Westheimer and McKee 1973; Ferman et al. 1987b); others conclude that Listing's law for pursuit movements is valid (Haslwanter et al. 1991; Tweed et al. 1992). Again, this discrepancy probably stems more from different ways of interpreting the data than from different experimental results: there seems to be disagreement about the level of eye deviation from Listing's plane that distinguishes nonspecific positional noise of the eye from clear-cut violations of Listing's law.

We therefore designed an experiment in which we directly compared the validity of Listing's law for fixations, saccades, and smooth pursuit eye movements made across the same eye positions in the orbit. For comparison we took data during blinks, since these movements provide an unequivocal example of a violation of Donders' and Listing's law (Ferman et al. 1987b). In the data analysis, we removed, in turn, long-term (minutes) fluctuation in torsion and any effects of bowing of Listing's plane to quantify the actual movement-induced torsional deviation from Listing's plane. Our aim was to study how much of the so-called thickness, i.e., the torsional variability, of Listing's plane was specifically induced by saccades, smooth pursuit movements, and blinks, but not by spontaneous fluctuations in torsion related to biological noise.

Materials and methods

Subjects

Five normal men (ages 32–50 years) were studied. Their visual acuities were 20/20 or better. Informed written consent was obtained after explanation of the experimental procedure, which was in accordance with the standards and with the approval of the Johns Hopkins Joint Committee on Clinical Investigation.

Eye movement recordings

Movements of the eyes about all three axes were simultaneously recorded from one eye (two subjects) or both eyes (three subjects) using dual search coils (Skalar, Delft, Netherlands). The field coil was built using a modification of the Remmel type system (Remmel 1984). It consists of a cubic coil frame of welded aluminum with a side length of 1.02 m, which produces three orthogonal magnetic fields with frequencies of 55.5, 83.3, and 42.6 kHz (intensities 0.088×10^{-4} tesla). Amplitude-modulated signals are identified using synchronous detection. The bandwidth is 0–90 Hz. Noise levels of the system were checked with a dual search coil fixed in the center of the coil frame; standard deviations were around 0.02° in the horizontal, vertical, and torsional directions.

Calibration procedures

Voltage offsets were nulled by connecting the search coils to the detector and then placing them in a metal tube that shielded the coils from the magnetic fields. Gains of the three magnetic fields were determined by mounting the connected coils on a gimbal and recording maximal induced voltages of each field. Details of the calibration procedure and the off-line computation of three-dimensional eye position are given elsewhere (Straumann et al. 1995).

Eye positions were expressed in rotation vectors, which describe the instantaneous orientation of the eye as a single rotation from the reference position. A rotation vector is oriented parallel to the axis of this rotation. Its length is defined by $\tan(\rho/2)$, where ρ is the angle of rotation (Haustein 1989). For convenience, we shall always give the rotation angle for each component in degrees. The coordinate system is determined by three head-fixed orthogonal axes with the *Z*-axis pointing upward, the *Y*-axis left-

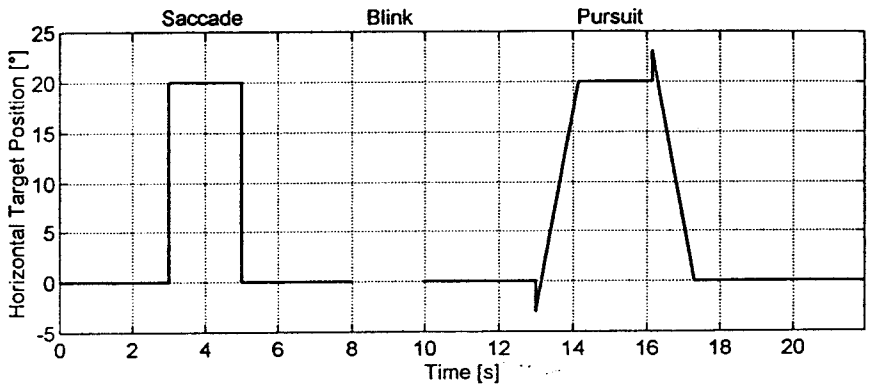

Fig. 1 Paradigm. The *bold line* indicates the horizontal position of the laser dot on the tangent screen as a function of time. When the light was turned off (interruption of bold line), the subject was asked to blink. The paradigm was repeated at different elevations of gaze to both sides. Periods of saccades (*Saccade*), blinks (*Blink*), and smooth pursuit movements (*Pursuit*) are indicated

ward, and the *X*-axis forward. According to the right-hand rule, positive eye movements about the *Z*-, *Y*-, and *X*-axis correspond to a leftward, downward, and clockwise rotation, respectively, as seen by the subject.

Experimental setup

Subjects were placed inside the coil frame so that the center of the interpupillary line coincided with the center of the frame. This was checked by a space-fixed laser beam projected to the center of the coil frame. During eye movement recordings, the head of the subject was immobilized with a bitebar. The position of the head was defined by the earth-horizontal orientation of the bitebar, which was checked by an inclinometer. After anesthetizing the conjunctiva with proparacaine HCl 0.5% (Ophthetic), dual search coils were mounted on one or both eyes.

During experiments, subjects were asked to fix upon a light dot (diameter 0.18°) which was back-projected by a laser onto a translucent tangent screen (distance from the center of the frame 124 cm) in otherwise complete darkness. The orientation of the laser was changed by two mirrors, which could be moved by galvanometers about the vertical or horizontal axis, respectively. The positions of the mirrors and the data collection were controlled by a personal computer. Voltages related to eye movements were digitized with a 12 bit A/D converter at 500 Hz and written to a hard disk. The data were analyzed off line in MATLAB (version 4.2c).

Possible coil artifacts

It has been suggested that long-term drifts (>20 s) of torsional coil signals are mainly due to torsional slippage of the annulus about the line of sight (Van Rijn et al. 1994; Straumann et al. 1995). Short-term torsional changes (in the range of 10–20 s), however, more closely reflect actual torsional eye position. This is supported by photographic recordings of eye torsion over time (Enright 1990; see also Discussion).

Another type of artifact in torsional eye position occurs when the coil abruptly slips during large saccades and blinks. It is our experience that in most subjects sudden torsional slippage is rare if the search coil is carefully mounted on the eye so that no air is allowed between the silicon annulus and the conjunctiva. Sudden torsional slips usually occur during the first 5 min after mounting the coil. During this initial period subjects performed fixation trials, which were not used for further analysis. In the analyzed database, we detected no clear instances of sudden torsional coil slippage.

Paradigm

Figure 1 shows the horizontal position of the light dot on the screen during a single trial, which consisted of a saccade followed by a pursuit stimulus. The stimulus started at a specific elevation along the vertical meridian and moved 20° to the right or left and back again. To induce constant smooth eye velocity but suppress catch-up saccades, the pursuit stimulus was of the Rashbass form (backward step, forward ramp) with a ramp velocity of 20°/s. During the interval with the saccadic and pursuit stimulus not moving the target was turned off, and the subject was asked to make a blink. Otherwise, trials with blinks during fixation, saccades, and smooth pursuit were eliminated from the analysis. If in an individual trial a steady fixation could not be maintained and the horizontal or vertical drift was more than 1°, the trial was also discarded. Trials were repeated five or six times to each side of the midline, at different elevations of gaze: −20°, −10°, 0°, 10°, and 20° with respect to the straight-head position. An experimental session with about 50 trials lasted 11 min.

Results

Figure 2 shows an example of an entire experimental session lasting 11 min (subject 3, left eye): rotation vectors of all trials at different elevations to each side are plotted in a frontal (Fig. 2A), side (Fig. 2C), top (Fig. 2D), and oblique projection (Fig. 2B). Each rotation vector describes the virtual rotation that would rotate the eye from the straight-ahead reference position to the instantaneous position. Note that the data cloud is somewhat tilted backward in the side projection (Fig. 2C), reflecting the fact that this subject's Listing's plane is not perpendicular to the chosen reference position straight-ahead (along the *x*-axis). Trajectories associated with blinks point to an absolute position 10° to the right (nasal) and 5° up (Fig. 2A, arrow). There is also a consistent blink-associated intorsional movement (Fig. 2D, arrow).

In Fig. 3 we plot the data of the previous figure as function of time and overlay all trials by aligning their onsets. The headings indicate the sections with centrifugal and centripetal saccades (Saccade), blinks (Blink), and centrifugal and centripetal smooth pursuit eye movements (Pursuit), respectively. In the top panel, which contains the torsional rotation vector components, a torsional deviation of the traces is seen whenever the eye is away from the vertical meridian in the lower panel. This effect is mainly due to the choice of reference position – in this case the straight-ahead position – which is not perpendicular to the best-fit plane through the data cloud (compare with the tilt of the data plotted in Fig. 2C). So, whenever the eyes move to the right or left, there is a

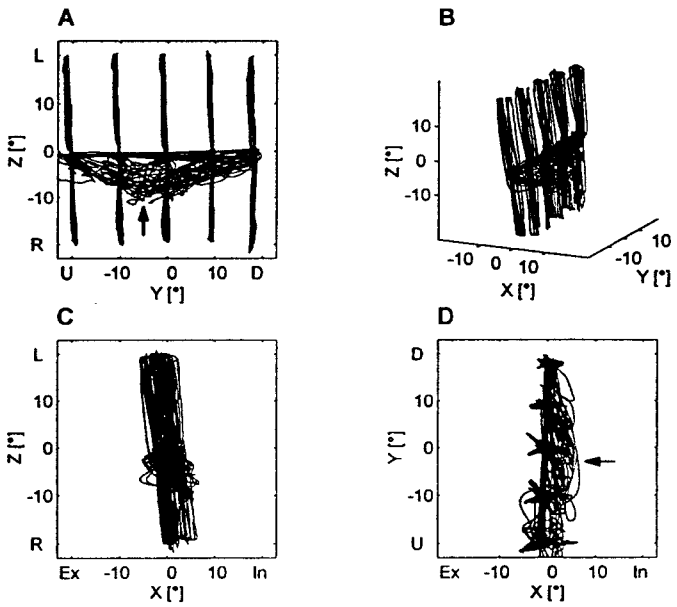

Fig. 2A–D Example of three-dimensional eye positions in rotation vectors (in degrees). Left eye of subject 3. The paradigm was repeated at 20°, 10°, 0°, −10°, and −20° elevation to each side of the vertical midline (amplitude 20°). The zero position, i.e., vector (0, 0, 0), coincides with the reference position straight-ahead. **A–D** show different projections of the coordinate system. *R* right (nasal), *L* left (temporal), *U* up, *D* down, *Ex* extorsion, *In* intorsion. **A** Frontal view (*Z–Y*-plane). *Arrow* indicates blink-associated right ward and upward movements. **B** Oblique view. **C** Side view (*Z–X*-plane). **D** Top view (*X–Y*-plane). *Arrow* indicates blink-associated intorsional components

cross-coupling with torsion in the positive or negative direction, respectively.

The first step of our analysis therefore consisted in a rotation of the data from each experimental session so that the best-fit plane through the points of fixation 200 ms *before* saccades, blinks, and pursuit movements were aligned with the *Z*- and *Y*-axes of the coordinate system. It must be stressed that we specifically did not take the entire data set to compute the best-fit plane, as Listing's law in its original formulation applies to fixations only. Because there are torsional drift movements following saccades (Enright 1986; Straumann et al. 1995), we did not include fixations *after* any ocular movement in the best-fit procedure. Fixation periods lasted about 3 s, so we were confident that post-movement torsional drifts had practically stopped at the beginning of the next movement (Enright 1986).

Figure 4 demonstrates the result of the rotation of the data. Now the so-called Listing's plane for fixations is aligned with the frontal plane of the coordinate system. The horizontal-torsional cross-coupling due to a non-primary reference position should now have vanished, unless the data points do not actually form a plane but rather a bowed surface. Independent of this issue, which will be addressed in the following paragraphs, the torsional scatter appears considerably larger than the scatter of the vertical and horizontal components, which agrees with the observation by others that torsion is less stable than horizontal and vertical eye position (Ferman et al. 1987a; Ott et al. 1992; Van Rijn et al. 1994). Also, some increased torsional thickness during the movements is apparent.

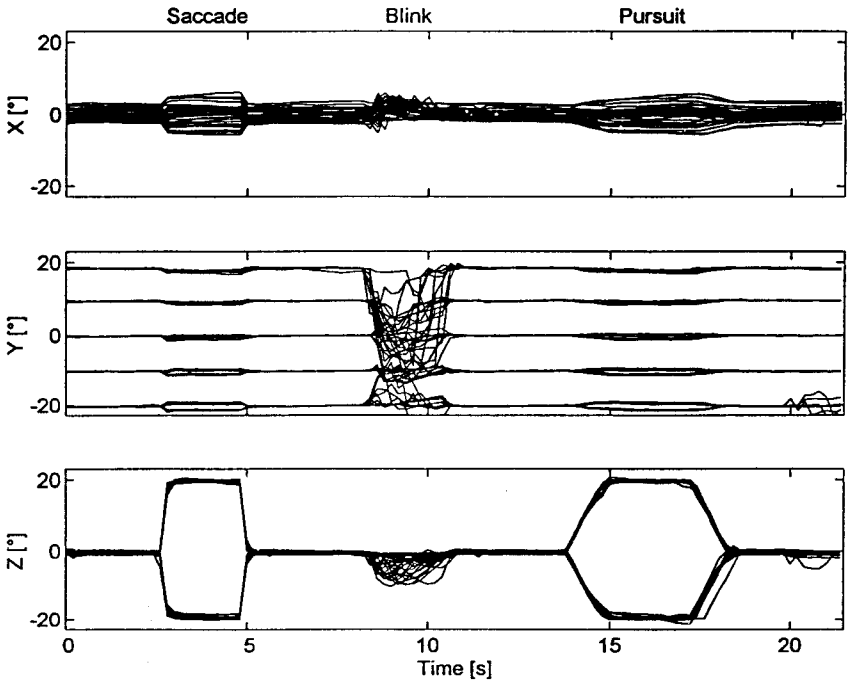

Fig. 3 Same data as in Fig. 2. Torsional (*X*), vertical (*Y*), and horizontal (*Z*) rotation vector components against time. *Saccade* section with centrifugal and centripetal saccades, *Blink* section with blinks, *Pursuit* section with centrifugal and centripetal smooth pursuit movements

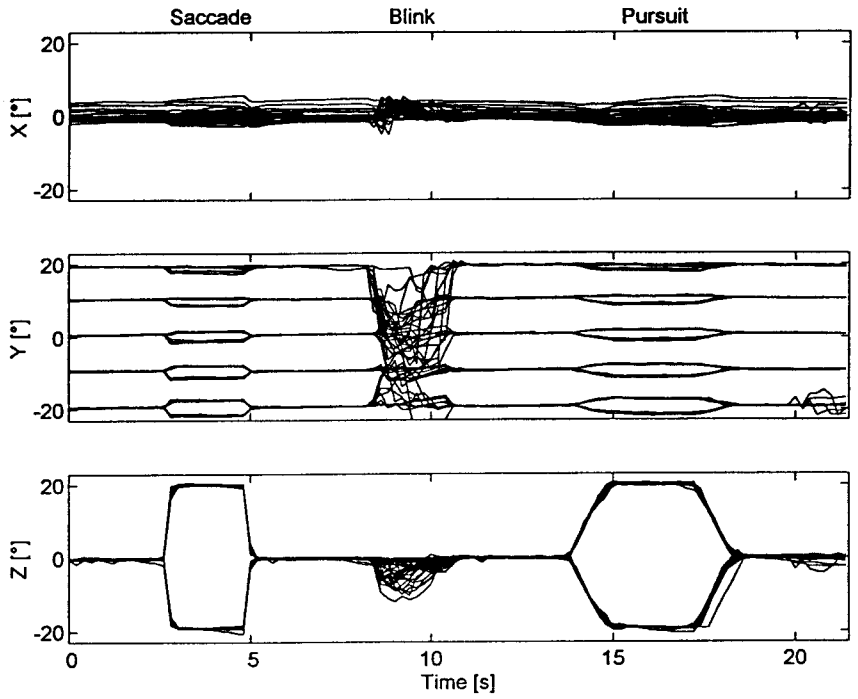

Fig. 4 Same data as in Figs. 2 and 3. Rotation vectors are rotated such that the best-fit plane of fixation points before movements aligns with the frontal plane of the coordinate system. For display purposes, rotation-induced shifts of horizontal and vertical trajectories are subtracted to let primary position coincide with the reference position straight-ahead on the screen

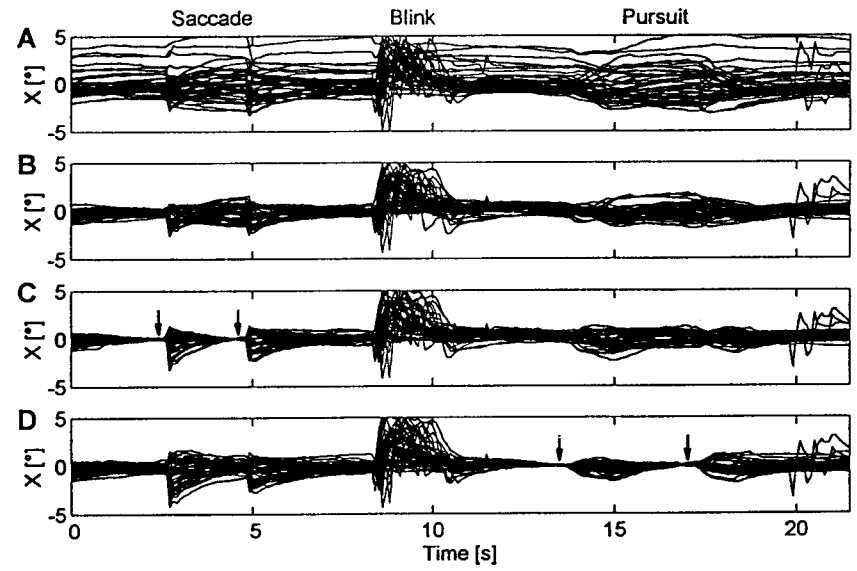

Fig. 5A–D Same data as in Figs. 2–4. Only the torsional components (X) of rotation vectors are shown. The rows **A–D** demonstrate the results of consecutive steps of data processing. **A** Data after aligning Listing's plane of the entire experimental session with the frontal plane of the coordinate system (enlargement of the first panel in Fig. 4). **B** Each trajectory is linearly detrended. **C** Each trajectory is rotated and shifted such that fixations before centrifugal and centripetal saccades are in a Listing's plane (*arrows*) which aligns with the frontal plane of the coordinate system. **D** Follows also step B. Same procedure as for step C, but Listing's plane is defined by fixations before centrifugal and centripetal smooth pursuit movements (*arrows*)

The next consecutive steps of analysis are summarized in Fig. 5, again using the same example as in Figs. 2–4:

(A) The first panel shows the overlay of torsional trajectories after the described rotational procedure (Fig. 5A, corresponds to the top panel of Fig. 4). The best-fit plane through the data cloud aligns with the Y–Z-plane of the coordinate system.
(B) From each torsional trajectory its linear trend is subtracted (Fig. 5B). Linear detrending consists of fitting a straight line through the data points scattered along the time axis and subtracting values on this line from corresponding data points at each sample period. The slope of the straight line corresponds to the net drift during the 21.5 s of the trial, and the offset represents the mean torsional offset during the trial. Linear detrending serves to subtract effects of long-term drifts in torsional eye position and does not influence movement-evoked torsional transients. It would also reduce increased torsional standard deviation due to bowing of the data cloud along the vertical direction. This issue will be discussed when presenting the quantitative analysis.
(C) Each trajectory is rotated and shifted such that the positions 200 ms before the centrifugal and centripetal saccades become zero (Fig. 5C, arrows). This corresponds to a reorientation of the trajectory into its individual Listing's plane defined by the two positions. The pro-

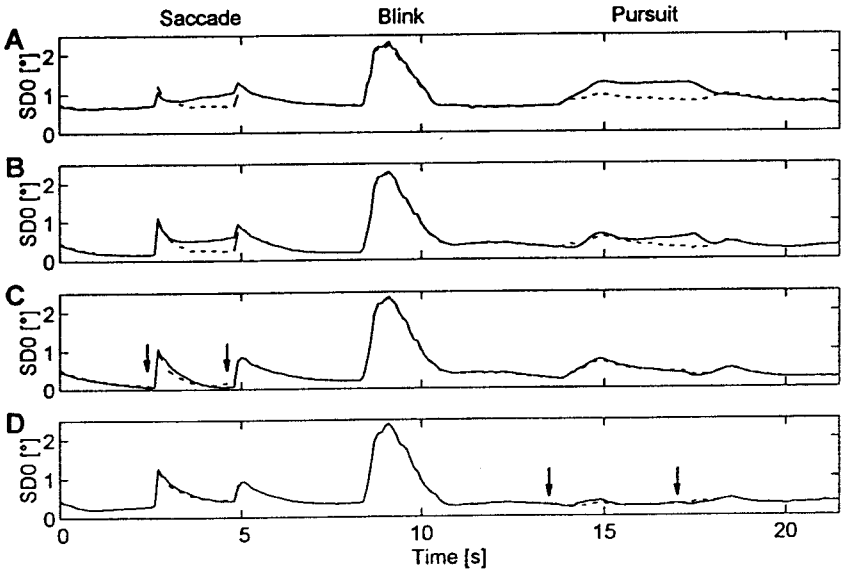

Fig. 6A–D Same data as in Figs. 2–5. Standard deviation from zero torsion (SD0) as a function of time. **A–D** and *arrows* correspond to Fig. 5. The *continuous line* indicates SD0 from a first-order best-fit surface (plane) through the data cloud of fixations; the *dashed line* represents SD0 from a second-order best-fit surface

cedure subtracts any torsional standard deviation due to a non-planar data cloud or to fluctuation in the orientation of Listing's plane over time.
(D) The same procedure as in step C is repeated. The positions that define Listing's plane, however, are chosen before the centrifugal and centripetal smooth pursuit eye movements (Fig. 5D, arrows).

In the following we shall call eye positions along the vertical meridian before a centrifugal and after a centripetal movement *quasi-secondary* (we use the prefix "quasi" because stimuli in the subject's midsagittal plane on the tangent screen only approximately coincide with secondary positions of the eye). Eye positions after centrifugal and before centripetal movements are *quasi-tertiary* (here we use the prefix "quasi" because one of the eccentric eye positions might coincide with a secondary horizontal position). In Fig. 5B the torsional scatter in quasi-tertiary positions appears considerably larger than that in quasi-secondary positions. This can be caused by a bowing of the surface formed by the data points, such that there is a cross-coupling between the horizontal and torsional rotation vector components. In the quantitative analysis (see below) we fitted the data points after each procedural step to second-order surfaces also, to explore how much of the torsional standard deviation in quasi-tertiary positions was due to bowing of the surface.

To quantify each of the four overlays, the standard deviation (SD0) from the best-fit plane (continuous line) or second-order surface (dashed line) through the data points of fixation was computed at each instant in time, as shown in Fig. 6 for this example. For the two fits we applied:

First order: $r_X = a_0 + a_1 r_Y + a_2 r_Z$
Second order: $r_X = a_0 + a_1 r_Y + a_2 r_Z + a_3 r_Y^2 + a_4 r_Y r_Z + a_5 r_Z^2$

where r_X, r_Y, r_Z are the torsional, vertical, and horizontal rotation vector components and $a_0 \ldots a_5$ the coefficients.

One can observe the following features:

(1) For quasi-secondary positions there is virtually no difference in SD0 after fitting first-order (plane) or second-order surfaces following each procedural step. This suggests that there is no vertical-torsional cross-coupling along the vertical meridian, i.e., no bowing of the surface along this line.
(2) After steps A and B there are marked differences in SD0 at quasi-tertiary eye positions between first- and second-order fitting. This implies horizontal-torsional cross-coupling for horizontal movements and therefore bowing of the surface in this direction. This observation agrees with data recently presented by DeSouza et al. (1995). To test whether the surfaces formed by the data points resemble more a plane, a Helmholtz or a Fick gimbal system, we fitted the following equation through the data clouds of fixations (Glenn and Vilis 1992):

$$s = \frac{r_X}{r_Y \cdot r_Z}$$

where r_X, r_Y, r_Z are the torsional, vertical, and horizontal position components of the rotation vectors and s the gimbal coefficient, whereby s=0 complies with Listing's law, s=1 with a Helmholtz, and s=−1 with a Fick gimbal. In the example shown we found coefficients s of 0.442, 0.234, −0.079, and −0.098 for steps A–D, respectively. Hence, the data after steps A and B tended to form a gimbal-like surface, which explains why in these panels (Fig. 6A, B) standard deviations from a first-order surface fit are larger in quasi-tertiary than in quasi-secondary positions.

(3) The main reduction in baseline SD0 was achieved by linear detrending (step B, Fig. 6B). Obviously, this procedure applied to a first-order fit does not eliminate the effects of bowed surfaces on the standard deviations in quasi-tertiary positions. It can, however, remove vertical-torsional cross-coupling for eye positions along the verti-

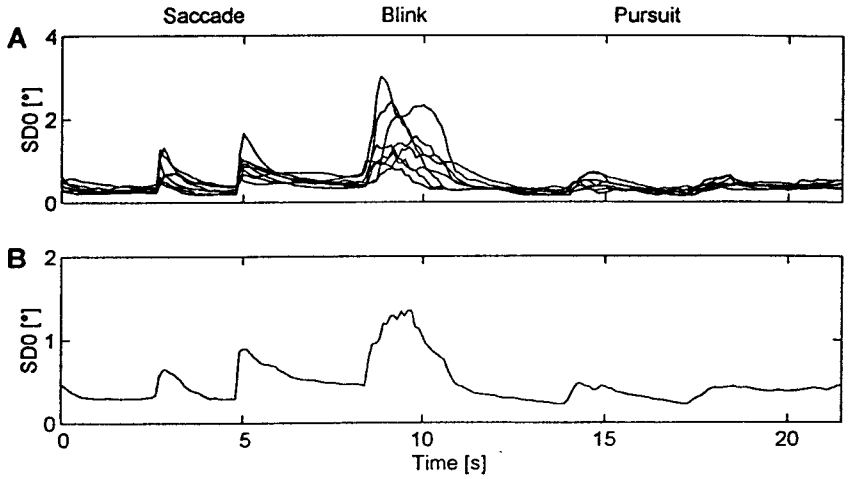

Fig. 7A, B Time course of standard deviations from zero torsion (SD0) in all measured eyes after step D. Corresponds to the example shown in Fig. 6D, continuous line. **A** SD0 traces of eight eyes. **B** Median SD0 trace of A

Table 1 Comparison of median values of SD0 (in degrees) over eight eyes (five subjects) during fixations in quasi-secondary vertical eye positions and quasi-tertiary eye positions

	Quasi-secondary eye position		Quasi-tertiary eye position	
	First-order surface: SD0 (°)	Second-order surface: SD0 (°)	First-order surface: SD0 (°)	Second-order surface: SD0 (°)
Step A	0.77	0.73	1.18	0.78
Step B	0.38	0.37	0.55	0.33
Step C	0.33	0.34	0.29	0.28
Step D	0.29	0.29	0.29	0.31

SD0 values are computed from first-order and second-order best-fit surfaces. Note that the largest differences between first- and second-order surfaces are found in quasi-tertiary eye positions after steps A and B

cal meridian (quasi-secondary positions). Since here we see no difference between the standard deviations of first- and second-order surface fits, bowing along this line is not present. Therefore linear detrending subtracts the increase in SD0 due to a trial-to-trial fluctuation of the torsional position of the eye.

(4) Standard deviations in quasi-tertiary positions after steps C or D (Fig. 6C, D) are the same whether we fit first- or second-order surfaces to the data. This means that determining individual Listing's planes for fixations in each trial eliminates both torsional cross-coupling effects due to bowing of the surface and trial-to-trial variations in torsion.

(5) The movement-evoked deviations from Listing's plane are largest for blinks, intermediate for saccades, and closest to the baseline SD0 for pursuit movements. Moreover, the relative saccade-evoked torsional standard deviation becomes larger after step B, as compared with the standard deviation during fixation.

Figure 7 gives an example on how the data of the eight eyes in five subjects were further reduced for the analysis of the entire data set. First, traces of SD0 from the best-fit plane (first-order surface) of step D, in which Listing's plane is defined before and after the centrifugal pursuit movements, are overlaid (Fig. 7A corresponds to Fig. 6D). Then, for each instant in time, the median value of the population is computed (Fig. 7B). Traces of medians are used for the quantitative description of the effects on scatter reduction by the different steps of analysis. The latter included fitting of both first- and second-order surfaces through the data clouds.

The following parameters were chosen for further analysis and computed for each analytical step over all eight eyes: (1) *baseline SD0*, (2) *peak saccade SD0*, (3) *peak blink SD0* and (4) *peak pursuit SD0*. The baseline SD0 was defined as the torsional standard deviation of quasi-tertiary positions just before the centripetal movements. For steps A and B we added the median SD0 values over all eyes before centripetal saccadic and pursuit movements, respectively, and divided it by two (average). For step C we took the median value before the pursuit, and for step D the median value before the saccadic centripetal movement. The reason for taking only one value in steps C and D was to eliminate any possible bias from a nearby subtraction of offsets. For the peak saccade and pursuit SD0 we added the medians over all eyes of the centrifugal and centripetal movements, respectively, and divided it by two (average).

Table 1 compares the baseline SD0 in quasi-tertiary positions with the corresponding values in secondary positions for the four analytical steps (medians over eight eyes). Results of fits for both first- and second-order surfaces are given. As already pointed out for a single example, values of first- and second-order fits are similar in quasi-secondary eye positions but differ for steps A

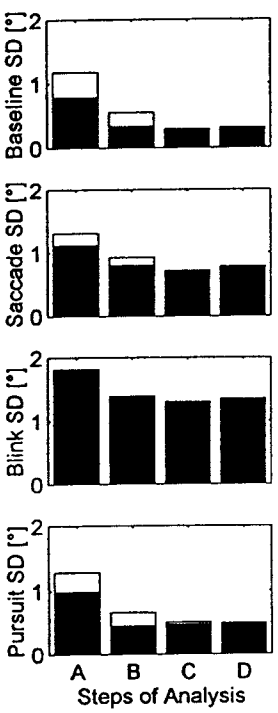

Fig. 8 Standard deviations (in degrees) from zero torsion (SD0) after steps of analysis A–D. For the eight eyes in five subjects the four panels show: *baseline SD0* (standard deviation of fixations in quasi-tertiary positions), *peak saccade SD0, peak blink SD0*, and *peak smooth pursuit SD0*. The categories on the *abscissa* denote the analytical steps A–D. *Open bars* SD0 from first-order best-fit surfaces (planes), *filled bars* SD0 from second-order best-fit surfaces. The SD0 values from the second-order surfaces were always smaller or almost equal to the SD0 values computed from a planar surface

and B in quasi-tertiary positions. Values for quasi-tertiary positions for steps C and D are almost identical. Gimbal coefficients s after step A were variable, but tended to a Helmholtz gimbal (mean=0.401, sd=0.427, min=−0.021, max=1.282, n=8 eyes).

Figure 8 summarizes the different SD0 values as a function of the procedural steps. The median values of the four parameters over eight eyes are shown as overlaid open (first-order fit) and filled (second-order fit) bars. The following features can be noted:

(1) A clear reduction in baseline SD0 by more than 50% is produced by the process of linear detrending (step B). For the first-order surfaces the reduction was 54%, for the second-order surfaces 58%. After linear detrending there was still a marked difference between baseline SD0 from both first- and second-order surface fits. More than half the standard deviation from the Listing's surface is therefore due to slow torsional drift that accumulates over the 11 min of the experimental session. This phenomenon has been named *long-term fluctuation* by Ferman et al. (1987a).

(2) Further mathematical manipulation by rotating each trajectory into its individual Listing's plane (steps C and D) decreased only the baseline SD0 of the first-order surface fit. In other words, this procedure mainly subtracted the effects of a curved Listing's surface. The residual scatter is therefore due to *short-term fluctuation* of torsional eye position in the range of a few seconds during fixations (Ferman et al. 1987a). The short-term fluctuation is not movement-induced since after saccades, blinks, and pursuit movements the baseline SD0 approaches its premovement level.

(3) As for the baseline SD0, the largest reductions in peak SD0 during saccades, blinks, and pursuit are observed when the data were linearly detrended (step B). The process of detrending assumes that all data points of fixation in the plane or surface are subject to the same long-term drift. The reduction in SD0 is less pronounced for saccades than for fixations; thus, the relative difference between the baseline SD0 of fixations and the peak saccade SD0 increases with steps B–D. The peak values of pursuit movements are always somewhat higher than the baseline SD0; both approximately decrease in parallel with the successive analytical steps.

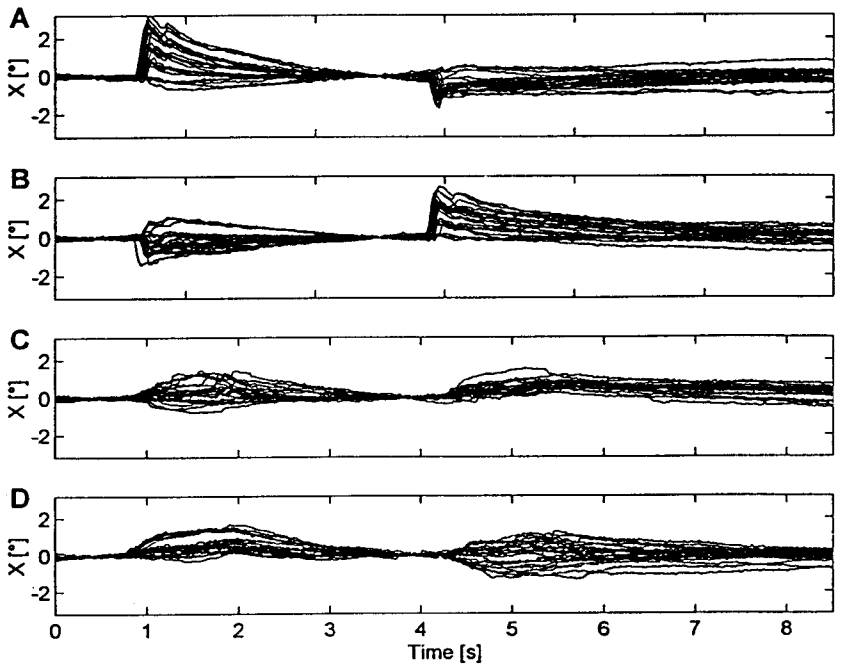

Fig. 9A–D Same data as in Figs. 2–6 (left eye of subject 3). Sections after analytical steps C (**A, B**) and D (**C, D**) are divided according to the direction of the centrifugal saccade. Only the torsional component (X) is shown. Left eye data are mirrored to the right eye. **A** Saccades to and from the temporal side. **B** Saccades to and from the nasal side. **C** Smooth pursuit movements to and from the temporal side. **D** Smooth pursuit movements to and from the nasal side

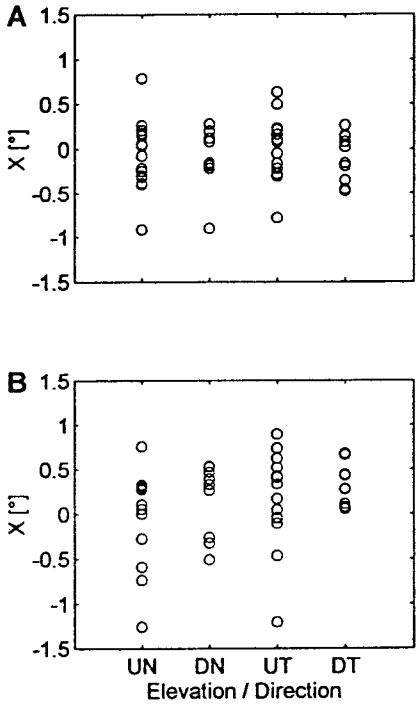

Fig. 10A, B Same data as in Figs. 2–6 and 9. *Data points* represent endpoints of traces in Fig. 9, which were further divided according to the elevation of gaze. *UN* "up/nasal" – gaze more than 8° above the reference position movements to and from the nasal hemifield, *DN* "down/nasal" – gaze more than 8° below the reference position etc., *UT* "up/temporal", *DT* "down/temporal". **A** Endpoints after saccades **B** Endpoints after pursuit movements

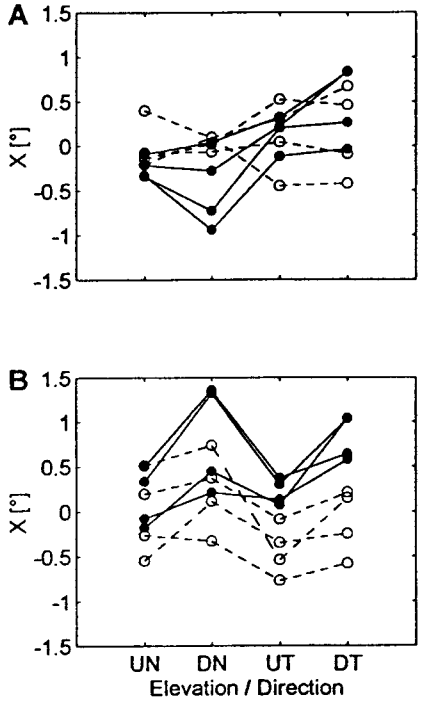

Fig. 11A, B Mean values (in degrees) of endpoints in the eight eyes, partitioned according to elevation of gaze and hemifield of movement. *Abbreviations* are explained in the legend of Fig. 10. *Filled circles* connected by *continuous lines* denote eyes in which data of the four groups (UN, DN, UT, DT) have significantly different means in the ANOVA test ($P<0.01$). *Open circles* connected by *dashed lines* denote eyes in which the ANOVA test showed no significant differences. **A** Endpoints after saccades. **B** Endpoints after pursuit movements

(4) Peak SD0 values after the last stage of the analytical procedures to reduce scatter (steps C or D) are more than 3 times the baseline value for blinks (first-order surface, 348% increase; second-order surface, 359% increase), more than twice the baseline value for saccades (first-order surface, 141% increase; second-order surface, 169% increase), and less than twice the baseline (first-order surface, 72% increase; second-order surface, 62% increase) for pursuit movements. The percentages in parentheses represent the mean of steps C and D for blinks, the value of step D for saccades, and the value of step C for pursuit movements.

Finally, we asked about the origin of the short-term fluctuation in baseline SD0, and specifically checked the hypothesis that the thickness of Listing's plane is a result of torsional hysteresis. This hypothesis was tested in the following way for saccades and pursuit movements:

(1) Trajectories that had been rotated in their individual Listing's planes (for saccades, step C; for pursuit movements, step D) were overlaid, and the endpoints of trajectories, well after the movement back to the vertical meridian, were taken for further analysis. Here we demonstrate the results for first-order surfaces; they were almost identical for second-order surfaces, since the standard deviations of both fits did not differ much after steps C and D (Fig. 8). Figure 9 shows examples of trajectories (left eye of subject 3) that were separated on the bases of whether the first movements occurred into the temporal (Fig. 9A, C) or nasal (Fig. 9B, D) direction. Left eye data were mirrored to the right eye, so that positive torsion was always extorsion.The torsional trajectories during saccades show the typical shape of torsional blips outlasting the end of the saccades (Fig. 9A, B) (Straumann et al. 1995).

(2) The endpoints of trajectories were further divided according to the elevation of gaze. Elevations above 8° from the straight-ahead position were included in the up-group, points below 8° were placed into the down-group. For the example given in the previous figure, the data distribution of the four groups are illustrated in Fig. 10. "Up-nasal" (UN), "down-nasal" (DN), "up-temporal" (UT), and "down-temporal" (DT) show considerable overlap for both saccades (A) and pursuit movements (B).

Figure 11 summarizes the statistical analysis of the eight eyes with respect to the distribution of data points in the four groups. Symbols denote mean values of data points for each group. In both the saccade and pursuit analysis, four eyes (filled circles connected by continuous lines) showed mean values that were significantly unequal in

Table 2 Corresponds to Fig. 11. For each eye the average standard deviation of endpoint groups and the standard deviation of all endpoints were computed (in degrees). Values for both saccadic and pursuit endpoints are given

Subject	Eye	Saccade		Pursuit	
		Average sd of groups	Overall sd	Average sd of groups	Overall sd
1	R	0.24	0.34	0.35	0.30
	L	0.28	0.34	0.33	0.43
2	R	0.35	0.32	0.44	0.35
	L	0.44	0.45	0.74	0.48
3	L	0.22	0.20	0.35	0.29
4	R	0.30	0.40	0.36	0.48
	L	0.30	0.34	0.27	0.45
5	R	0.38	0.37	0.40	0.35
Mean		0.31	0.34	0.41	0.39

the ANOVA test ($P<0.01$). This suggests a torsional hysteresis effect. Only two eyes were significantly unequal in both the saccade and pursuit ANOVA analysis.

To quantify the impact of different means of the four groups on the baseline standard deviation after the centripetal movement, we compared the standard deviations of endpoints in the individual groups with the overall standard deviation. Note that in this case we were not concerned with the deviation from Listing's plane (SD0) but with the standard deviation from the average value of data sets (sd). Table 2 compares the average sd values in the four groups with the sd value of all endpoints. The data demonstrate that, for saccades, sd is only slightly increased if one pools all endpoints in each subject. For pursuit movements there is no increase at all. This finding implies that movement directions and elevation of gaze during the movements have little effect on the thickness of Listing's plane for fixations after the effects of long-term drift and bowing of the surface have been eliminated.

Discussion

Our aim was to quantify the different sources of the so-called thickness of Listing's plane. In five normal subjects, three of whom were recorded binocularly, we tried to differentiate long-term (over minutes) and short-term (over seconds) torsional fluctuations of the eyes (Ferman et al. 1987a) from increased torsional scatter due to movements. The experimental paradigm consisted of centrifugal and centripetal horizontal saccadic and pursuit movements to both sides at different elevations of gaze. Between movements subjects were asked to fixate or blink. As a measure of scatter we took the standard deviation of data points (SD0) from Listing's plane or a second-order Listing's surface.

Four parameters were specifically analyzed: baseline SD0 during fixations in tertiary positions, peak SD0 during 20° saccades, peak SD0 during blinks, and peak SD0 during 20° pursuit movements with 20°/s ramps. By linearly detrending individual trajectories, containing fixations and movements, at a specific elevation and in a specific direction (duration 21.5 s), we found that more than 50% of the baseline SD0 during an 11-min trial was due to long-term fluctuations in torsion, independent of whether a first- or second-order surface was fitted through the data cloud of eye rotation vectors. Median baseline SD0 of tertiary positions across all eyes before detrending was 1.18° from a first-order and 0.78° from a second-order surface (Fig. 8, first panel, step A), which is somewhat less than standard deviations of 1.2–2.1° for consecutive primary positions reported by Ferman et al. (1987a). Since SD0 values of fixations along the tangent screen's vertical meridian were almost identical for first- and second-order fits of the data before linear detrending (Table 1) and the difference in SD0 baseline from a first- and second-order surface were little changed by this procedure, we concluded that linear detrending subtracted the effects of long-term drift and not the effects of possible vertical-torsional cross-coupling due to bowing of the Listing's surface along vertical secondary eye positions.

As pointed out by Van Rijn et al. (1994), long-term torsional fluctuation may well reflect torsional coil slippage on the conjunctiva. With binocular recordings, these authors found presumably nonphysiological accumulation of cyclovergence (2–4°) during experimental sessions (duration about 15 min), which they attributed to blinks with the upper lid touching the wire-leads of the coils. In the three subjects in whom we measured eye movements binocularly, we found similar increases in cyclovergence over time. Consistent with this notion that long-term torsional fluctuation is mainly a coil artifact, Enright (1990) showed, using a photographic method, that the standard deviations of torsion during 30 sequential fixations was only 18 min arc.

Further data processing in which each trajectory was rotated into its individual Listing's plane decreased only the remaining baseline SD0 from a first-order surface; hence this procedure subtracted the effects of horizontal-torsional cross-coupling due to bowing of the Listing's surface, which tended to resemble a Helmholtz gimbal in most subjects. Whether this observation is of any physiological significance remains open (DeSouza et al. 1995).

After this last latter procedural step, the baseline SD0 remained around 0.3–0.4°. This value agrees well with the short-term fluctuation in torsion measured during 15 s (Ott et al. 1992) or 32 s (Van Rijn et al. 1994) of fixation straight ahead with a standard deviation of about

0.2°. For fixations during 4 s, torsional SD0 values around 0.15° have been reported (Ferman et al. 1987a). An interval of 4 s is probably not long enough for the SD0 of the short-term fluctuation to saturate, which would be the reason why this value is less than the SD0 value measured in our experiments. In fact, systematic computation of torsional variability as a function of time during straight-ahead fixation shows a plateau after 10–20 s (Van Rijn et al. 1994).

Since, in this study, eye movements were restricted to the horizontal direction, we cannot address the question whether mixing points of fixation after horizontal and vertical movements would lead to a further increase in thickness of Listing's plane, as has recently been suggested by DeSouza et al. (1995). These authors reported that fixations after horizontal or vertical saccades are distributed on different second-order surfaces; consequently the combined population of data points showed a larger standard deviation from the overall surface. However, as we have shown in this paper, this cannot be the only reason why Listing's plane is thick.

High-resolution video recordings of eye position after centripetal horizontal saccades have demonstrated torsional hysteresis (Enright 1986). Using dual search coils, Ferman et al. (1987b) reported that by stepping the eyes around primary position with a radius of 20° or more, torsional components during fixations of identical points show differences of 1–2°, depending on whether the eyes circled in a clockwise or counterclockwise direction, which also suggests torsional hysteresis. We therefore asked whether or not part of the measured standard deviation during fixations, after removing long-term fluctuations, might be due to hysteresis. Analyses of torsional endpoints after consecutive horizontal back-and-forth movements at different elevations of gaze and to both sides showed that the impact of torsional hysteresis on the standard deviation from Listing's plane can be neglected. Note that we cannot exclude the possibility that hysteresis effects might contribute to the thickness of Listing's plane after vertical eye movements.

One of the main reasons for the renewed interest in Listing's and Donders' laws is related to whether or not these laws also apply to eye positions during movements and are not restricted to the static situation. A frequently used measure for the validity of Listing's law is the standard deviation of all analyzed data points in different secondary and tertiary eye positions from a first-order plane fit through the data cloud. Since the relative increase in standard deviation of eye position during saccades was small (about 30%), it was concluded that Listing's law is valid during saccades (Tweed and Vilis 1990). In our analysis, however, we detrended each trajectory (duration 21.5 s) to eliminate effects of long-term drift and rotated it into its individual Listing's plane, since the overall Listing's surface is not totally flat. When we re-computed the standard deviation of fixations in tertiary positions from Listing's plane (SD0 from first-order surface) after these rotations, its relative increase during blinks was 348%, during saccades 141%, and during pursuit 72%. We consider these numbers as more appropriate measures of the validity of Listing's law during movements. Our results indicate that Listing's law was violated not only during blinks and saccades, but also during pursuit movements.

At this point, we can only speculate why Listing's law is not observed during eye movements (Straumann et al. 1995): a possible reason is that the velocity command for saccadic and pursuit eye movements has only a horizontal and vertical component. Due to the non-commutativity of rotations, this would lead to transient torsional movements out of Listing's plane with passive drifts back to zero torsion after the movement (Schnabolk and Raphan 1994). In this case, violations of Listing's law would be a function of the amplitude of the velocity command, which could explain why standard deviations from Listing's plane during pursuit are smaller than during saccades. Alternatively, or in addition, the mechanical properties of the plant, e.g., eye muscle pulling directions, might provide an explanation for the deviations from Listing's plane during movements (Demer et al. 1995). Another factor may be that during saccades the antagonist eye muscle signal is driven into inhibitory cutoff. This could lead to a change in mechanical forces and might explain why Listing's law is violated more during saccades than during pursuit eye movements. In the absence of a quantitative dynamical plant model, however, we cannot speculate further on such mechanisms.

We want to stress that in this study the three-dimensional analysis of ocular movements was at the level of eye position. Deviations of ocular positions from Listing's law, however, also imply deviations of angular eye velocity vectors from the so-called half-angle strategy. This kinematic rule states that the *instantaneous* angular velocity vector tilts by half the angle of gaze, if position is restricted to Listing's plane (Tweed and Vilis 1990). The deviation of angular eye velocity from the half-angle strategy reflects the dynamics and magnitude of the torsional blip during an eye displacement (for saccades: see Tweed and Vilis 1990, Fig. 2). If both the starting and ending positions are in Listing's plane, then the *average* angular velocity vector of a movement will obey the half-angle rule even if the saccade contains a torsional blip. This mathematical truism, however, does not mean that the saccade generator itself produces signals in accordance with the half-angle strategy.

In conclusion, we were able to show that spontaneous fluctuations in torsion, bowing of Listing's surface, and movement-evoked deviations from Listing's plane are independent phenomena. Since movement-evoked torsional transients during and after horizontal saccades agree with high-resolution video recordings of post-saccadic torsional drift (Enright 1986), we are confident that they are not due to slippage of the search coil on the eye (Straumann et al. 1995). Increased variability of torsion during eye movements therefore represents violations of Listing's law and cannot simply be interpreted by an imprecision in the control of torsional eye position: in reality, static eye positions, i.e. fixations, appear extremely well controlled by Listing's law, if we take into account

some bowing of the surface, while movements show clear deviations. This raises doubts about the existence of a so-called *internal Listing's law operator for eye movements* as proposed by others (Crawford and Vilis 1995). It rather seems that Listing's law is implemented only at the level of position coding, possibly by the ocular motor velocity-to-position integrator, and not in the velocity signals to the eye plant. We would like to suggest that future three-dimensional kinematical studies in normal subjects and in patients should differentiate between movement-induced deviations from Listing's plane and deviations produced by physiological or coil-related short- and long-term torsional fluctuations.

Acknowledgements We are grateful for the technical assistance provided by A.G. Lasker and D.C. Roberts. We would also like to thank V. Henn for helpful remarks. One referee's comments led to important clarifications and improvements of the manuscript. This work was supported by Schweizerische Stiftung für medizinisch-biologische Stipendien, NIH EY01849, and a Manpower Award from Research to Prevent Blindness.

References

Crawford JD, Vilis T (1995) How do motor systems deal with the problems of controlling three-dimensional rotations? J Mot Behav 27:89–99

Demer JL, Miller JM, Poukens V, Vinters HV, Glasgow BJ (1995) Evidence for fibromuscular pulleys of the recti extraocular muscles. Invest Ophthalmol Vis Sci 36:1125–1136

DeSouza JFX, Mikael S, Nicolle DA, Vilis T (1995) Why is Listing's plane thick? Soc Neurosci Abstr 21:1199

Donders FC (1848) Beiträge zur Lehre von den Bewegungen des menschlichen Auges. Holländische Beiträge Anat Physiol Wiss 1:105–145

Enright JT (1986) The aftermath of horizontal saccades: saccadic retraction and cyclotorsion. Vision Res 26:1807–1814

Enright JT (1990) Stereopsis, cyclotorsional "noise" and the apparent vertical. Vision Res 20:1487–1497

Ferman L, Collewijn H, Van den Berg AV (1987a) A direct test of Listing's law. I. Human ocular torsion measured in static tertiary positions. Vision Res 27:929–938

Ferman L, Collewijn H, Van den Berg AV (1987b) A direct test of Listing's law. II. Human ocular torsion measured under dynamic conditions. Vision Res 27:939–951

Glenn B, Vilis T (1992) Violations of Listing's law after large eye and head gaze shifts. J Neurophysiol 68:309–318

Haslwanter T, Straumann D, Hepp K, Hess BJM, Henn V (1991) Smooth pursuit eye movements obey Listing's law in the monkey. Exp Brain Res 87:470–472

Haustein W (1989) Considerations on Listing's law and the primary position by means of a matrix description of eye position control. Biol Cybern 60:411-420

Helmholtz Hv (1867) Handbuch der Physiologischen Optik. Voss, Hamburg

Minken AWH, Van Opstal AJ, Van Gisbergen JAM (1993) Three-dimensional analysis of strongly curved saccades elicited by double-step stimuli. Exp Brain Res 93:521–533

Ott D, Seidman SH, Leigh RJ (1992) The stability of human eye orientation during visual fixation. Neurosci Lett 142:183–186

Remmel RS (1984) An inexpensive eye movement monitor using the scleral search coil technique. IEEE Trans Biomed Eng 31:388–390

Ruete CGT (1853) Lehrbuch der Ophthalmologie. Braunschweig, pp 36–37

Schnabolk C, Raphan T (1994) Modeling three-dimensional velocity-to-position transformation in oculomotor control. J Neurophysiol 71:623–638

Straumann D, Haslwanter T, Hepp-Reymond MC, Hepp K (1991) Listing's law for eye, head and arm movements and their synergistic control. Exp Brain Res 86:209–215

Straumann D, Zee DS, Solomon D, Lasker AG, Roberts D (1995) Transient torsion during and after saccades. Vision Res 35:3321–3334

Tweed D, Vilis T (1987) Implications of rotational kinematics for the oculomotor system in three dimensions. J Neurophysiol 58:832–849

Tweed D, Vilis T (1990) Geometric relations of eye position and velocity vectors during saccades. Vision Res 30:111–127

Tweed D, Fetter M, Andreadaki S, Koenig E, Dichgans J (1992) Three-dimensional properties of human pursuit eye movements. Vision Res 32:1225–1238

Tweed D, Misslicsh H, Fetter M (1994) Testing models of the oculomotor velocity to position transformation. J Neurophysiol 72:1425–1429

Van Rijn LJ, Van der Steen J, Collewijn H (1994) Instability of ocular torsion during fixation: cyclovergence is more stable than cycloversion. Vision Res 34:1077–1087

Westheimer G (1989) Saccadic eye movements as a control system: history and methodology. In: Wurtz RH, Goldberg ME (eds) The neurobiology of saccadic eye movements. Elsevier, Amsterdam, pp 3–12

Westheimer G, McKee SP (1973) Failure of Donders' law during smooth pursuit eye movements. Vision Res 13:2145–2153